



HHS Public Access

Author manuscript

Otol Neurotol. Author manuscript; available in PMC 2019 September 01.

Published in final edited form as:

Otol Neurotol. 2018 September ; 39(8): e654–e659. doi:10.1097/MAO.0000000000001906.

Intra-Cochlear Electrocochleography during Cochlear Implant Electrode Insertion is Predictive of Final Scalar Location

K Koka¹, WJ Riggs², R Dwyer³, JT Holder³, JH Noble³, BM Dawant³, A Ortmann⁴, C Valenzuela⁴, JK Mattingly², MS Harris⁵, BP O'Connell⁶, LM Litvak¹, OF Adunka², CA Buchman⁴, and RF Labadie³

¹Research and Technology, Advance Bionics Corp., Valencia, CA

²Department of Otolaryngology- Head and Neck Surgery, The Ohio State University, Columbus, OH

³Department of Otolaryngology- Head and Neck Surgery, Vanderbilt University and Medical Center, Nashville, TN

⁴Department of Otolaryngology- Head and Neck Surgery, Washington University School of Medicine, St. Louis, MO

⁵Department of Otolaryngology and Communication Sciences, Medical College of Wisconsin, Milwaukee, WI

⁶Department of Otolaryngology-Head and Neck Surgery, University of North Carolina, Chapel Hill, NC

Abstract

HYPOTHESIS: Electrocochleography (ECoChG) patterns observed during cochlear implant (CI) electrode insertion may provide information about scalar location of the electrode array.

BACKGROUND: Conventional CI surgery is performed without actively monitoring auditory function and potential damage to intracochlear structures. The central hypothesis of this study was that ECoChG obtained directly through the CI may be used to estimate intracochlear electrode position and, ultimately, residual hearing preservation.

METHODS: Intracochlear ECoChG was performed on 32 patients across 3 different implant centers. During electrode insertion, a 50-ms tone burst stimulus (500 Hz) was delivered at 110 dB SPL. The ECoChG response was monitored from the apical-most electrode. The amplitude and phase changes of the first harmonic were imported into an algorithm in an attempt to predict the intracochlear electrode location (scala tympani (ST), translocation from ST to scala vestibuli (SV), or interaction with basilar membrane). Anatomic electrode position was verified using post-operative computed tomography (CT) with image processing.

RESULTS: CT analysis confirmed 25 electrodes with ST position and 7 electrode arrays translocating from ST into SV. The ECoChG algorithm correctly estimated electrode position in 26

Disclosures: KK and LL are employees of Advanced Bionics Corp. OFA, CAB, RFL are consultants for Advanced Bionics Corp, Med-El Corp, Cochlear Corporation and MSH is a consultant with Advanced Bionics Corp. OFA and CAB have an ownership interest in Advanced Cochlear Diagnostics, LLC.

(82%) of 32 subjects while 6 (18%) electrodes were wrongly identified as translocated (sensitivity=100%, specificity=77%, positive predictive value=54%, and a negative predictive value=100%). Greater hearing loss was observed postoperatively in participants with translocated electrode arrays (36 ± 15 dB) when compared to isolated ST insertions (28 ± 20 dB HL). This result however, was not significant ($p=0.789$).

CONCLUSION: Intracochlear ECochG may provide information about CI electrode location and hearing preservation.

Keywords

cochlear implantation; scalar translocation; electrocochleography (ECochG); ECochG; Scala Tympani (ST); Scala Vestibuli (SV)

INTRODUCTION

Cochlear implantation (CI) is the standard of care for adults and children with severe-to-profound sensorineural hearing loss (SNHL). CI surgery that achieves electrode placement exclusively within ST can result in hearing preservation and improved performance. In cases of residual low frequency hearing, it has been demonstrated that preservation of residual inner ear structures by means of proper location of the electrode array may result in preservation of residual pre-operative hearing important for achieving optimal performance following implantation (1–6). Preservation of residual hearing is becoming more and more important as the number of patients who are candidates of electro-acoustic stimulation (EAS) strategies continues to increase.

Modifications in surgical technique (e.g., round window insertion) (7), electrode design (e.g., lateral wall) (8,9), and the use of pharmacologic agents (e.g. steroids) (10) have all been employed to increase the likelihood for successful hearing preservation. However, conventional CI surgery is performed without a means of monitoring the physiologic integrity of the inner ear structures during manual insertion of the electrode array. One such monitoring technique is electrocochleography (ECochG) which can provide real-time feedback from the inner ear structures, specifically the hair cells, and spiral ganglion cells. Furthermore, as we explore in this paper, ECochG may provide an indication of scalar location during and after electrode insertion. Given that scala tympani (ST) insertion without crossover into scala vestibule (SV) has been associated with better hearing outcomes (11) and estimates of rate of translocation from ST into SV as high as 32% (5,8), such a predictive alarm could be clinically useful.

Recent reports have attempted to explore the utility of electrocochleography (ECochG) as a method for detecting functionally relevant, micromechanical changes within the cochlea during CI surgery. The ECochG response includes electrophysiological signatures that reflect hair cell activation (i.e., the cochlear microphonic (CM))(12) and can be recorded from both extracochlear and intracochlear locations. The latter approach has used the CI electrodes as a means of monitoring intracochlear trauma resulting from array insertion (13–18). O’Connell et al., (18) demonstrated significant differences between exclusive ST insertions and those translocating from ST to SV using intra-operative, post-insertion

ECochG and post-operative audiometry. However, these reports were limited by their inability to identifying scalar location of the electrode. The goal of this study was to determine how the ECochG pattern(s) observed during CI electrode insertion could provide information about scalar location of the electrode array and potentially predict hearing preservation.

METHODS

Institutional Review Board (IRB) approval was obtained at all participating institutions. Adult CI candidates with normal labyrinthine anatomy and without middle ear disease or history of prior ear surgery who had chosen an Advanced Bionics HiRes90K Advantage implant with a HiFocus Mid Scala electrode (Valencia, CA), were eligible for study inclusion. All participants provided separate written consents for surgery and study participation.

Intraoperative Technique

Following anesthetic induction, a foam-tipped sound tube was placed in the external auditory meatus, and the pinna was gently folded forward, as previously described (19). Care was taken not to crimp the sound tube. Following incision, a cortical mastoidectomy followed by facial recess and round window niche removal was carried out. After placement of the receiver-stimulator within the periosteal pocket, the implant head-piece was aligned with the internal device and held in place, magnetically. The surgeon then proceeded with a round window (RW) or extended RW cochlear entry.

Electrocochleography

The ECochG apparatus and custom software (Advanced Bionics Corp., Valencia, CA) was used to record the ECochG responses from the apical electrode contact during insertion of the array (16). An alternating polarity 500 Hz tone burst stimulus (50 ms) was delivered at 110 dB SPL during electrode insertion. Notations were made by the person running the ECochG software regarding depth of insertion of the electrode array including initial entry into the cochlea and at various locations as verbally specified by the implanting surgeon (e.g. electrode 4 at RW, proximal blue line at RW, distal blue line at RW). Responses were recorded at ~ 4–5 averages/sec.

Data Analysis

Fast Fourier transformation (FFT) (Mathworks, Natick, MA) was used to obtain the amplitude and phase of the first harmonic response during the insertion. The amplitudes were converted to dB (re: 1 uV). The amplitude and phase patterns at the first harmonic during insertion were then categorized in an effort to predict the scalar electrode location. These observed changes were categorized as either same scalar location (ST) or translocation (ST/SV). These scalar locations were estimated through various predictive algorithms applied to the ECochG responses recorded during insertion. This algorithm had been formulated based on a training set of ECochG recordings from prior work (16–18) and focused on both amplitude and phase of the ECochG signal. Note that amplitude changes are presented as dB (dB relative to amplitude at RW) with the caveat that dB does not refer to

audiological levels as is typical in an audiogram but rather represents an order of magnitude change in response (e.g. 20 dB refers to an increase from 1mV to 10mV and 6 dB refers to an increase from 1 mV to 2mV). Phase difference refers to the change between the acoustic signal presented via the ear insert and the recorded ECoChG signal with the acoustic signal typically leading, thus eliciting the ECoChG response.

The ECoChG responses were classified according to the 3 distinct patterns shown in Fig. 1. The amplitude and phase characteristics of **Type 1** was an overall increase in amplitude and small changes in phase from start of insertion to end of insertion. The **Type 2** pattern was distinguished by an increase in amplitude during insertion followed by a drop in amplitude at the end of insertion with a large change in phase at or near complete inversion (180 degrees or π radians) during the drop in amplitude. The **Type 3** pattern was distinguished by an increase in amplitude during insertion followed by sharp drop in amplitude but a smaller phase change during the drop in amplitude. An empirical algorithm was developed with standard amplitude drop and phase change to differentiate between these three patterns. First author (KK), who was blinded to the CT scan results, observed the insertion tracks for each patient and categorized the ECoChG response as one of these three patterns based on the empirical algorithm.

Post-insertion CT Scan

CT scans were obtained following electrode insertion either in the operating room or following surgery. Analysis was carried out according to previous described protocols (20–21).

RESULTS

Reconstructed CT images of two representative participants are shown in Figure 2. Panels A and B show a representative participant with an electrode array that did not translocate during insertion. Panel C shows the amplitude and ECoChG phase responses during this insertion. A Type 1 pattern is demonstrated showing an increase in the amplitude of the response during insertion followed by a small decrease and plateau. Overall phase changes of approximately 3 radians (~180 deg) from the beginning to the end of insertion were observed. A 13 dB decrease in low frequency pure tone average (PTA, average of 125, 250 and 500 Hz) was verified at the first fitting appointment, approximately 4 weeks after surgery. This participant has an insertion angle of 345 degrees. Panels D and E show the reconstructed images for a representative participant with an electrode array that translocated from ST to SV during insertion. Panel F shows the amplitude and phase of the ECoChG responses illustrating a Type 3 response with an initial increase in the amplitude of the response followed by a sharp decrease. Small changes in phase during the drop in amplitude were observed. A PTA change of 37 dB at the first fitting appointment, approximately 4 weeks after surgery was observed. This participant has an insertion angle of 416 degrees.

Table 1 shows the results of behavioral audiometric testing, CT scan determined electrode location, angular insertion depth, and ECoChG patterns for the 32 implanted subjects. Post-operative CT scans revealed that 25 of the 32 participants (78%) had electrode arrays that resided completely in the ST throughout the insertion and 7 participants (22%) that had

electrode arrays that translocated from ST to SV at some point during insertion. Post-operative PTA was higher amongst the group with confirmed translocation (36 ± 15 dB loss) when compared to those with electrodes confined to ST (28 ± 20 dB loss). This difference was not significant ($p=0.789$).

AMPLITUDE/PHASE PATTERNS:

Based on the ECoChG patterns observed during the insertion, the participants were divided into two groups: same scalar insertion (i.e. non-translocation) or translocation. Type 1 patterns were treated as same scalar insertion, i.e. ST or SV only. The increase in amplitude of the ECoChG suggests that the electrode imparts minimal trauma on intracochlear structures while reaching the apical portions of the cochlea where residual hearing is most likely to be present. Type 2 patterns characterized by an initial increase in amplitude followed by a large reduction in amplitude and a large phase change were also treated as same scalar insertion. Type 3 patterns characterized by initial amplitude rise followed by amplitude drop along with small phase change were treated as scalar translocations.. Table 1 shows the scalar estimation based on ECoChG responses and CT scan scalar identification. The ECoChG algorithm correctly estimated electrode position in 26 (82%) of 32 subjects while 6 (18%) electrodes were wrongly identified as translocated (sensitivity=100%, specificity=77%, positive predictive value=54%, and a negative predictive value=100%).

DISCUSSION

The results of the current study suggest that the amplitude and phase of intracochlear ECoChG recordings can be used to predict the final scalar location of a CI electrode array. Our empirical algorithm correctly identified final intracochlear electrode location (i.e., same scala (ST or SV only) versus ST/SV translocation) in 81% of the cases in this sample of 32 adult CI recipients. The six cases that represent false negative predictions of final scalar location (i.e., the algorithm predicted electrodes translocating from ST to SV, but translocation was not demonstrated according to CT) provide insight into possible situations which likely change the basilar membrane mechanics, e.g. the CI electrode touching or pushing upon basilar membrane but not resulting in true translocation.

The current study is the first to look at ECoChG amplitude and phase changes during insertion to estimate scalar location of the electrode array and verify through CT scans. Interpreting ECoChG amplitude and phase changes during CI electrode insertion is complex due to the fact that the recording electrode is being moved from the base to apex, and amplitude and phase are known to vary according to location within the cochlea. In 1953, Von Békésy (23) reported that maximal displacement of the basilar membrane is frequency and location dependent. In 1975, Wilson and Johnstone et al., (24) showed intracochlear place dependent phase changes in which phase, with respect to the stimulus at the tympanic membrane, increased from base to apex. Frequency specific phase changes or delays have been previously reported either using ABR or extracochlear ECoChG (25–26). More recently, Campbell et al., (27) used intra-cochlear multi-electrode ECoChG after CI array insertion to demonstrate that delay of ECoChG gets progressively larger from the base to the apex similar to traveling wave properties described in earlier literature.

Previous work by Campbell and colleagues (15, and 27), provided preliminary data for the notion that ECoChG insertion patterns with a sizeable decrease in the CM magnitude during insertion without recovery indicates intracochlear trauma. The data contained herein are in agreement with these findings as all of the cases with a translocation demonstrated a drop in CM magnitude without recovery. The current work builds from this starting point by demonstrating that the incorporation of phase characteristics with amplitude allows better specificity and sensitivity when predicting scalar translocation based on ECoChG analysis. Specifically, our algorithm interprets a large phase change—nearly completely out of phase at 180 degrees or π radians—to indicate the electrode array has not translocated while smaller phase changes would indicate translocation.

It is not entirely clear to us why the phase shift is so important in predicting scalar location. The phase shift represents a discontinuity between the leading signal, the acoustic stimulus presented via the ear insert at 500Hz, and the lagging signal, the ECoChG recording. Our initial interpretation was that large phase shifts would be associated with translocation signaling the dissociation of the signals. However, the training algorithm differentiated between large phase shifts, those approximating 180 degrees (π radians) and smaller phase shifts. Exploring the prior literature, we have formulated a hypothesis that the large phase shift, or inversion, may be associated with normal functioning of the basilar membrane perhaps associated with recordings in near proximity to the characteristic frequency (CF) of the basilar membrane for the 500Hz acoustic signal. This hypothesis is supported by the work of Kohloffel et al. (22) who recorded ECoChG amplitude and phase in an animal model and showed phase changes of approximately 180 degrees and drops in amplitude when the recording electrode moved past the CF region. However, the 500Hz region of the basilar membrane is typically beyond the reach of CI electrodes (30). Our algorithm indicates that phase changes not near the complete inversion range of 180 degrees are associated with translocation perhaps indicating a random dissociation between the leading and training signals. This contention is supported by prior animal work (28, 29). While these initial results are promising for clinical applicability, understanding the nuances of patient specific ECoChG recordings will require many additional data sets.

CONCLUSION

Real-time ECoChG recorded through the CI electrode array likely provides the implanting surgeon feedback with information predictive of the location of the electrode array within the cochlea.

ACKNOWLEDGEMENTS

The authors would like to thank all of the subjects who participated in the study. This research was supported by the National Institute of Health (NIH, R01DC008408, R01DC014462, R01DC014037 and T32DC00022).

REFERENCES

1. Aschendorff A , Kromeier J , Klenzner T et al. Quality control after insertion of the nucleus contour and contour advance electrode in adults. *Ear Hear* 2007; 28:75S–9S. [PubMed: 17496653]
2. Finley CC , Holden TA , Holden LK et al. Role of electrode placement as a contributor to variability in cochlear implant outcomes. *Otol Neurotol* 2008; 29:920–8. [PubMed: 18667935]

3. Carlson ML , Driscoll CL , Gifford RH et al. Implications of minimizing trauma during conventional cochlear implantation. *Otol Neurotol* 2011; 32:962–8. [PubMed: 21659922]
4. Holden LK , Finley CC , Firszt JB et al. Factors Affecting Open-Set Word Recognition in Adults With Cochlear Implants. *Ear Hear* 2013.
5. O'Connell BP , Cakir A , Hunter JB et al. Electrode Location and Angular Insertion Depth Are Predictors of Audiologic Outcomes in Cochlear Implantation. *Otol Neurotol* 2016; 37:1016–23. [PubMed: 27348391]
6. Gantz BJ , Turner C , Gfeller KE et al. Preservation of hearing in cochlear implant surgery: advantages of combined electrical and acoustical speech processing. *Laryngoscope* 2005; 115:796–802. [PubMed: 15867642]
7. Adunka O , Unkelbach MH , Mack M et al. Cochlear implantation via the round window membrane minimizes trauma to cochlear structures: a histologically controlled insertion study. *Acta Otolaryngol* 2004; 124:807–12. [PubMed: 15370564]
8. Wanna GB , Noble JH , Carlson ML et al. Impact of electrode design and surgical approach on scalar location and cochlear implant outcomes. *Laryngoscope* 2015 *Otol Neurotol*. 2015 9; 36(8): 1343–8.
9. Boyer E , Karkas A , Attye A et al. Scalar localization by cone-beam computed tomography of cochlear implant carriers: a comparative study between straight and periomodiolar precurved electrode arrays. *Otol Neurotol* 2015; 36:422–9. [PubMed: 25575374]
10. Sweeney AD , Carlson ML , Zuniga MG et al. Impact of Perioperative Oral Steroid Use on Low-frequency Hearing Preservation After Cochlear Implantation. *Otol Neurotol* 2015; 36:1480–5. [PubMed: 26375969]
11. Wanna GB , Noble JH , Gifford RH et al., Impact of Intrascalar Electrode Location, Electrode Type, and Angular Insertion Depth on Residual Hearing in Cochlear Implant Patients: Preliminary Results. *Otol Neurotol*. 2015 9; 36(8):1343–8. [PubMed: 26176556]
12. Dallos P , Cheatham MA . Production of cochlear potentials by inner and outer hair cells. *J Acoust Soc Am* 1976; 60:510–2. [PubMed: 993471]
13. Dalbert A , Sim JH , Gerig R et al. Correlation of Electrophysiological Properties and Hearing Preservation in Cochlear Implant Patients. *Otol Neurotol* 2015; 36:1172–80. [PubMed: 25839980]
14. Campbell L , Kaicer A , Briggs R et al. Cochlear response telemetry: intracochlear electrocochleography via cochlear implant neural response telemetry pilot study results. *Otol Neurotol* 2015; 36(3):399–405. [PubMed: 25473960]
15. Campbell L , Kaicer A , Sly D et al. Intraoperative Real-time Cochlear Response Telemetry Predicts Hearing Preservation in Cochlear Implantation. *Otol Neurotol* 2016; 37:332–8. [PubMed: 26859542]
16. Harris MS , Riggs WJ , Giardina CK et al. Patterns Seen During Electrode Insertion Using Intracochlear Electrocochleography Obtained Directly Through a Cochlear Implant. *Otol Neurotol* 2017; 38:1415–20. [PubMed: 28953607]
17. Harris MS , Riggs WJ , Koka K et al. Real-Time Intracochlear Electrocochleography Obtained Directly Through a Cochlear Implant. *Otol Neurotol* 2017; 38:107–13.
18. O'Connell BP , Holder JT , Dwyer RT et al. Intra- and Postoperative Electrocochleography May Be Predictive of Final Electrode Position and Postoperative Hearing Preservation. *Frontiers in Neuroscience*, 2017, 11(May), 1–12. [PubMed: 28154520]
19. Adunka OF , Giardina CK , Formeister EJ et al., Round window electrocochleography before and after cochlear implant electrode insertion. *Laryngoscope*. 2016 5; 126(5):1193–200. [PubMed: 26360623]
20. Teymouri J , Hullar TE , Holden TA et al., Verification of computed tomographic estimates of cochlear implant array position: a micro-CT and histologic analysis. *Otol Neurotol*. 2011 8; 32(6): 980–6. [PubMed: 21725264]
21. Schuman TA , Noble JH , Wright CG et al., Anatomic verification of a novel method for precise intrascalar localization of cochlear implant electrodes in adult temporal bones using clinically available computed tomography. *Laryngoscope*. 2010 11; 120(11):2277–83. [PubMed: 20939074]
22. Kohlöffel L (1970). Longitudinal amplitude and phase distribution of the cochlear microphonic (guinea pig) and spatial filtering. *Journal of Sound and Vibration*, 11, 325–334.19.

23. Von Békésy G : Description of some mechanical properties of the organ of Corti. *J Acoust Soc Am* 1953; 25: 770–785.
24. Wilson JP , Johnstone JR : Basilar membrane and middle-ear vibration in guinea pig measured by capacitive probe. *J Acoust Soc Am* 1975; 57: 705–723. [PubMed: 1123489]
25. Eggermont JJ : Narrow-band AP latencies in normal and recruiting human ears. *J Acoust Soc Am* 1979; 65: 463–470. [PubMed: 489815]
26. Schoonhoven R , Prijs VF , Schneider S : DPOAE group delays versus electrophysiological measures of cochlear delay in normal human ears. *J Acoust Soc Am* 2001; 109: 1503–1512. [PubMed: 11325122]
27. Campbell L , Bester C , Iseli C , Sly D et al.,. Electrophysiological Evidence of the Basilar-Membrane Travelling Wave and Frequency Place Coding of Sound in Cochlear Implant Recipients. *Audiology & Neuro-Otology*, 2017, 22(3), 180–189. [PubMed: 29084395]
28. Littler TS , *The Physics of the Ear*, Pergamon Press, 1965.
29. Davis H , Fernandez C , McAuliffe DR . The excitatory process in the cochlea. *Proc Natl Acad Sci U S A*. 1950 10; 36(10):580–7. [PubMed: 14808143]
30. Greenwood DD : A cochlear frequency-position function for several species – 29 years later. *J Acoust Soc Am* 1990; 87: 2592–2605. [PubMed: 2373794]

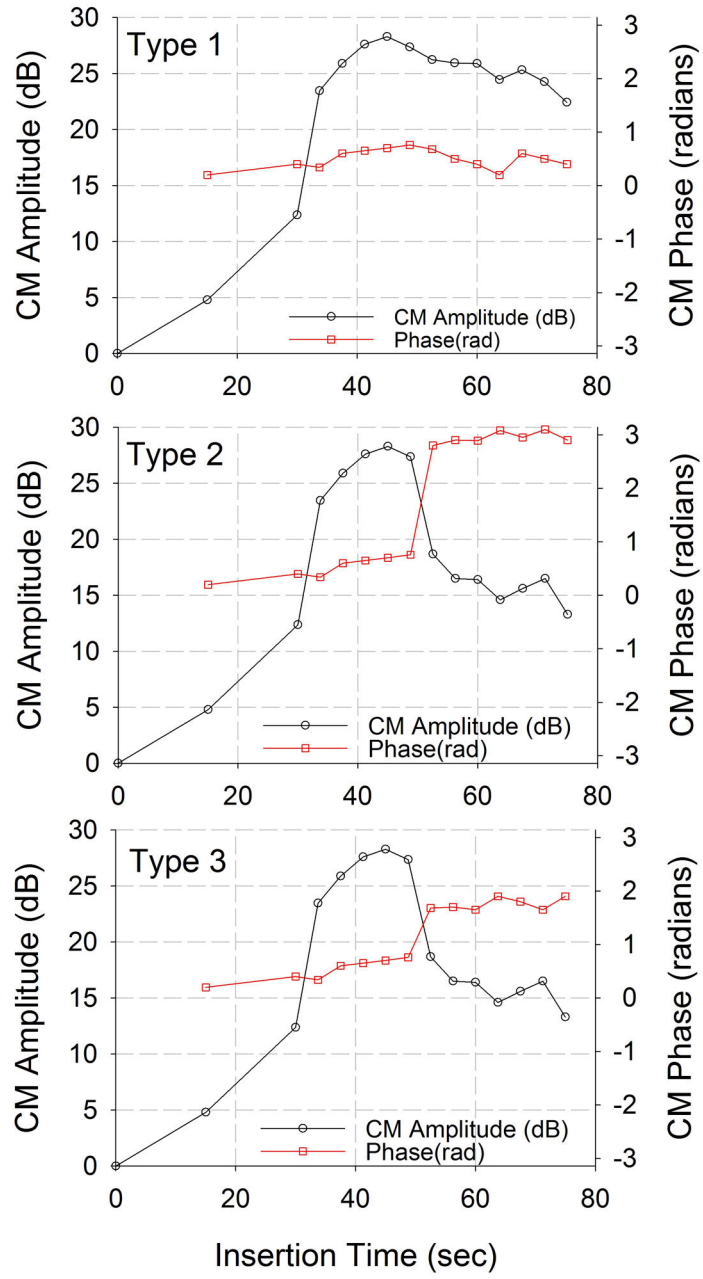


Figure 1: Simulated patterns observed during insertion for amplitude and phase.

Author Manuscript

Author Manuscript

Author Manuscript

Author Manuscript

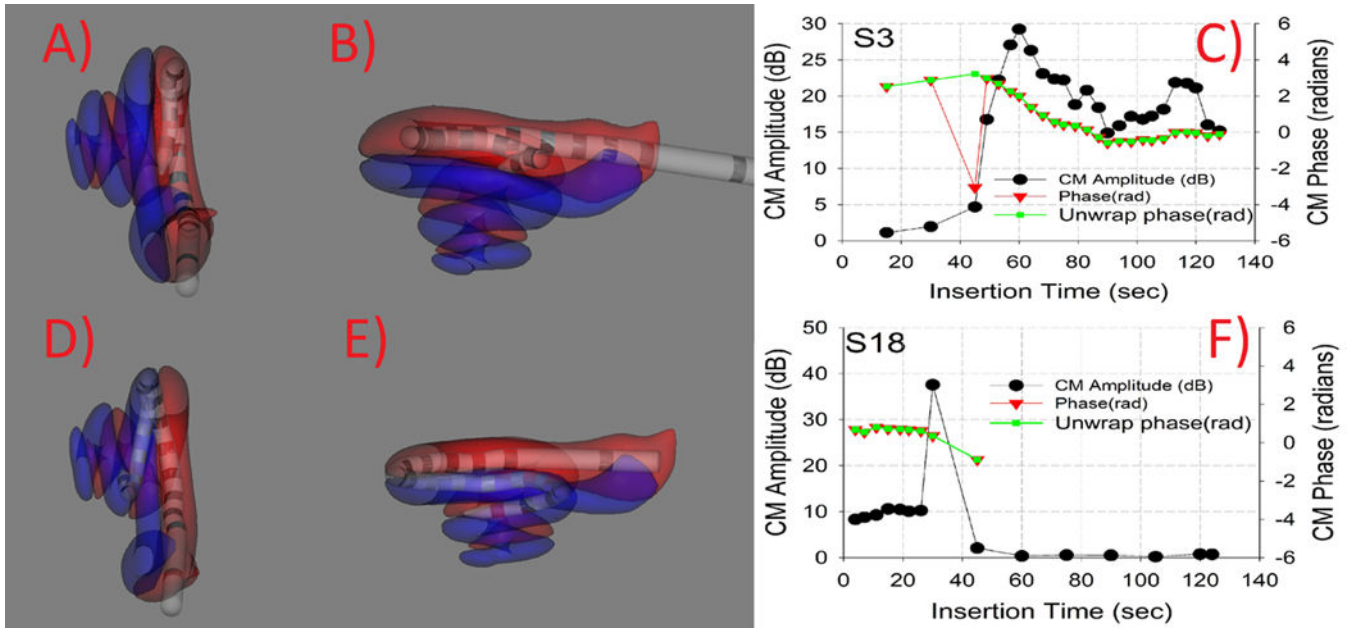


Figure 2:

Two representative insertions for each non-translocation and translocation. Panels A and B show two different views of a reconstructed CT image showing insertion completely in ST. Panel C shows the ECoHG amplitude and phase changes during insertion. ECoHG amplitudes show increase during insertion and minor decrease in amplitude during insertion. Panels D and E show two different views of reconstructed CT image showing electrode translocation from ST to SV. Panel F shows the ECoHG amplitude and phase changes during insertion. ECoHG amplitude shows an increase in amplitude followed by a dramatic drop and no recovery.

Table 1

Scalar location estimation through CT and ECoChG

Subject ID	PTA Change	CT Scalar Location	Insertion Angle (CT)	ECoChG Scalar Estimation	ECoChG Insertion Type
S1	0	ST	339	ST	1
S2	22	ST	340	ST	2
S3	13	ST	345	ST	1
S4	24	ST	349	ST	2
S5	43	ST	368	SV	3
S6	8	ST	411	ST	1
S7	37	ST	340	ST	1
S8	7	ST	393	ST	1
S9	34	ST	408	ST	1
S10	59	ST	348	ST	1
S11	21	ST	375	SV	3
S12	43	ST	357	ST	1
S13	4	ST	381	ST	1
S14	26	ST	371	ST	1
S15	35	SV	322	SV	3
S16	47	SV	395	SV	3
S17	43	SV	414	SV	3
S18	37	SV	416	SV	3
S19	53	SV	368	SV	3
S20	39	ST	375	SV	3
S21	3	ST	326	ST	2
S22	20	ST	396	SV	3
S23	65	ST	389	ST	1
S24	24	ST	350	ST	1
S25	50	ST	344	ST	1
S26	29	ST	423	ST	1
S27	10	SV	439	SV	3
S28	34	ST	372	SV	3
S29	70	ST	404	ST	1
S30	DNT	ST	483	ST	1
S31	25	SV		SV	3
S32	20	ST		SV	3